

GeO₂ Nanowires Doped with Optically Active Ions

Pedro Hidalgo, Emanuela Liberti, Yamilet Rodríguez-Lazcano, Bianchi Méndez,* and Javier Piqueras

Departamento de Física de Materiales, Facultad de Ciencias Físicas, Universidad Complutense de Madrid, 28040 Madrid, Spain

Received: June 15, 2009; Revised Manuscript Received: August 21, 2009

GeO₂ nanowires doped with Eu, Er, or Mn, as well as codoped with each of these ions and Sn, have been grown by a catalyst-free vapor–solid process. The incorporation of Sn has been found, in all cases, to favor the formation of straight wires, which make them more appropriate for waveguiding purposes. Cathodoluminescence (CL) in the scanning electron microscope (SEM) has been used to investigate the complex light emission from the nanowires. Rare earth ion emission lines and defect related bands have been observed in Eu- and Er-doped nanowires. Optical coupling and waveguiding behavior of Er-doped GeO₂ nanowires have been demonstrated for green laser light and for Er excited luminescence in the wires. In Mn-doped GeO₂ nanowires a band centered at 1.75 eV had been detected. X-ray photoemission measurements show the presence of GeO oxide in the surface of the GeO₂ wires, which influences their native defect structure.

GeO₂ is a transparent conductive oxide (TCO) with a high potential in optoelectronics. Its band gap energy (5 eV), higher than other TCO materials, makes this oxide attractive as host for optical impurities to develop luminescent devices, from the ultraviolet-blue to the near-infrared range. As in the case of other oxides, GeO₂ nanowires are potentially useful in nanoelectronic applications or optical nanodevices.^{1,2} In particular, its rather high refractive index (around 2) enables GeO₂ nanowires to act as waveguides in the visible range, and the physical properties of GeO₂ nanowires may be tuned by doping with suitable impurities. Rare earths (REs) and metal transition elements have been long studied in several wide band gap semiconductor hosts to modify optical and magnetic properties. For example, Er³⁺ ions have been extensively used as luminescent centers in silicon and silicon oxides in an attempt to make efficient luminescent silicon-based devices^{3,4} and Eu³⁺ ions have been used as luminescent ions in other wide band gap semiconductors, such as GaN films.^{5–7} Germanium-based systems, such as germanosilicates, Si–Ge alloys, or GeO₂ glasses, have been explored as hosts for RE ions in order to reach greater optoelectronic integration. GeO₂ has been studied as an alternative host material for planar waveguides due to its low phonon energies, which would lead to an improvement of quantum efficiency and the rather high solubility for RE dopants compared to SiO₂.⁸ GeO₂, as other semiconductor oxides, has oxygen deficiency associated to its high concentration of oxygen vacancies, and this effect is more acute in nanowires due to the higher surface–volume ratio. These defects are, in many cases, responsible for their smart optical and electrical properties and are the key factor in order to exploit them in practical devices, such as sensors or optoelectronic devices. Doping of semiconductor oxide nanostructures is an expanding field with unresolved problems, such as the interplay between native defects with impurities or the difficulty to achieve efficient impurity solubility in crystalline nanowires. On the other hand, metal ions usually introduce localized states in the forbidden band gap and they may form

bonds with oxygen vacancies, modifying the defect structure in the nanowires, and hence influencing their luminescence properties. Doping of semiconductor oxide nanowires with luminescent-sensitive ions has been reported, as for instance Er in SnO₂,⁹ Eu in Ga₂O₃,¹⁰ or Eu in ZnO.¹¹ Er-doped GeO₂ nanowires grown by a catalyst assisted vapor–liquid–solid (VLS) process have been also recently reported.¹²

In this work, luminescence properties of GeO₂ nanowires, grown by a catalyst-free thermal method, doped with several elements are investigated. The impurities are both RE ions (Er and Eu) and metal impurities (Sn and Mn). The doped nanowires have been characterized by X-ray diffraction (XRD), scanning electron microscopy (SEM), cathodoluminescence (CL) in the SEM, X-ray energy dispersive spectroscopy in SEM and X-ray photoelectron spectroscopy (XPS). Light waveguiding experiments have been performed with the aid of an optical microscope.

GeO₂ nanowires were obtained from compacted Ge powder by a vapor–solid process in an open furnace as described elsewhere.² The doping impurities used in this work are Sn, Mn, Er, and Eu. The starting materials used were high-purity Ge powder and the corresponding metal oxide powder (4–5% at. of SnO₂, Mn₂O₃, Er₂O₃, or Eu₂O₃). The precursor powders were prepared by milling the corresponding mixture in a ball mill (Retsch S100) with 20 mm agate balls for 5 h. Disk-shaped samples of about 7 mm diameter and 2 mm thickness were made under compressive load of powders and were then annealed at 600 °C for 6 h under an argon flow of 0.2 sccm. After the thermal treatment, the surface of the disk is full covered by GeO₂ nanowires. This method does not use a foreign catalyst and enables to grow doped GeO₂ nanowires in a single-step process by the addition of doping elements into the initial powder. The structural properties of the nanowires were studied by XRD. The morphology of the nanostructures was characterized by SEM in a FEI Inspect S microscope. A Bruker energy dispersive X-ray microanalysis system and a CL setup were both implemented into a SEM Leica 440 Stereoscan microscope, which enables us to perform compositional and luminescence studies with high spatial resolution. CL spectra in the SEM were recorded either with a Hamamatsu R5509 cooled photomultiplier

* To whom correspondence should be addressed. E-mail: bianchi@fis.ucm.es.

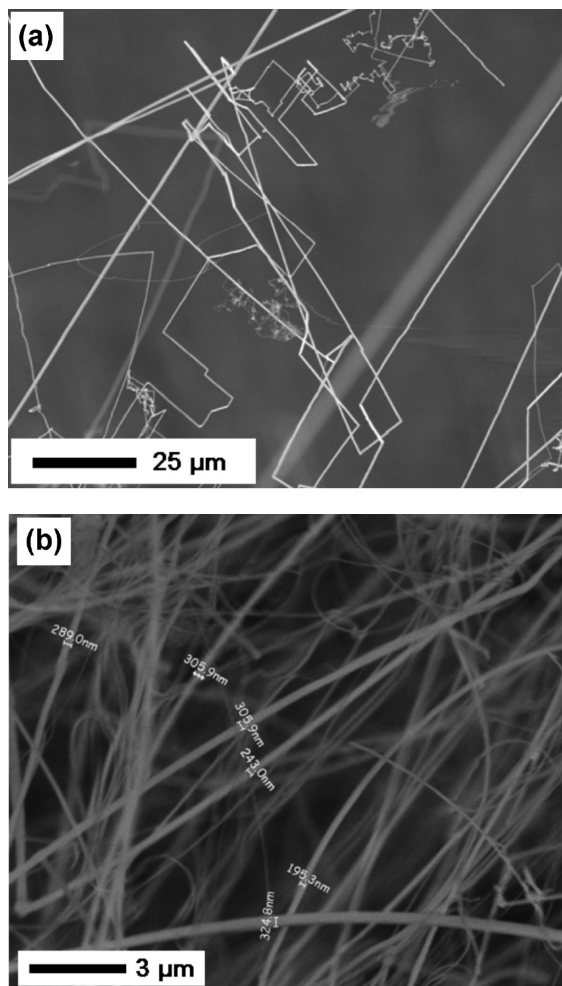


Figure 1. Representative SEM image of (a) Mn-doped GeO₂ nanowires and (b) Sn-codoped GeO₂:Mn nanowires.

or with a Hamamatsu PMA-11 charge couple device camera. For the waveguiding experiments, nanowires were glued at the end of a commercial light guide of 100 μm diameter and a 535 nm green laser light was used as illumination source. A Hamamatsu R-928 photomultiplier tube operating in the photon counting mode was used as light detector. Spatially resolved XPS measurements were performed at the ESCA microscopy beamline of the Elettra synchrotron facility in Trieste. The scanning photoelectron microscope (SPEM) can work in both imaging and spectroscopy mode by using a zone plate focusing optics which produces a microprobe with a diameter of 0.15 μm . Photoemission spectra were measured by using 646 eV photon energy X-ray with a 0.2 eV energy resolution.

Undoped GeO₂ nanowires grown by the above-described procedure usually show a high aspect ratio with widths of 200–400 nm and lengths of several hundred micrometers. Also, a rather high percentage of these wires exhibit bends of around 90° possibly due to crystallographic defects, such as twins.² Figure 1a shows representative SEM micrographs of Mn-doped GeO₂ wires, which reveal the formation of very long wires with the presence of sharp bends. Similar morphology features are observed in Er- and Eu-doped GeO₂ nanowires. In a previous work, we have shown that the addition of a small amount (2.5% at.) of SnO₂ into the initial Ge mixture leads to the growth of a higher density of GeO₂ nanowires that are thinner and have less bends than in the Sn-free case.¹³ For this reason, we have added Sn oxide in the precursor pellet, which leads to the formation of Sn-codoped GeO₂ nanowires without, or only

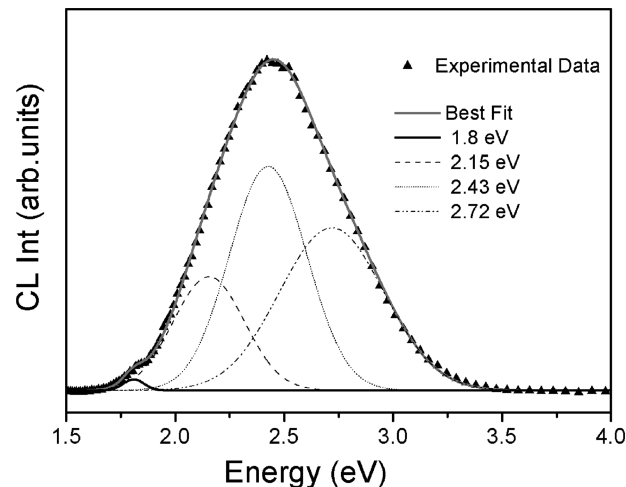


Figure 2. CL spectrum of undoped GeO₂ nanowires.

occasionally observed, bends. Figure 1b shows a SEM micrograph of Sn-codoped GeO₂:Mn nanowires of widths in the range 150–300 nm and almost free of bends. The same procedure has been followed for Eu and Er doping of GeO₂ nanowires and the Sn-codoped wires show similar morphology.

In all doped samples studied in this work, the main diffraction peaks recorded in XRD spectra correspond with α -GeO₂ phase maxima from nanowires and pure Ge phase from the substrate. For each particular doping case, maxima peaks of europium oxide, erbium oxide, and manganese oxide from the substrate are also recorded in the XRD spectra. The growth process of doped nanowires involves oxidation of the Ge substrate and impurities diffusion into the nanowires. To avoid the contribution of substrate, EDX spectra measurements were performed on the nanowires grown on the rim of the pellets and confirmed the presence of doping element in each case, with concentrations in the range of 1 and 2% at.

Figure 2 shows the CL spectrum of undoped GeO₂ nanowires, with a broad green band centered at 2.4 eV. Gaussian deconvolution of the band shows the four components (1.9, 2.17, 2.42, and 2.70 eV) that best fit the experimental data. Similar CL spectrum is obtained in the case of S-doped GeO₂ nanowires. CL studies of GeO₂ crystals have reported a green band in GeO₂ quartz-like and glassy crystals, attributed to oxygen deficient centers.³ In other cases, luminescence from GeO₂ has been investigated in relation with the emission in Ge nanocrystals surrounded by an oxide layer.¹⁵ Green-orange photoluminescence of GeO₂ has also been reported in Ge nanocrystals embedded in GeO_x ($0 < x < 2$) thin films^{16,17} or in a SiO₂ matrix.¹⁸ In most of the cases, the luminescence has been discussed in terms of the presence of Ge–O centers related to oxygen vacancies. The complex luminescence band observed in the GeO₂ nanowires suggests that vacancy defects occur in several configurations and/or forming complex defects. Moreover, as the entangled wires have a large surface–volume ratio compared with films, surface states may also be involved in the luminescence properties of GeO₂ nanowires. Besides that, in order to study the influence of impurities in the GeO₂ nanowires luminescence the interplay between Sn and dopant in codoped samples and the possible modification of native defects must be taken into account.

The main visible Eu³⁺ emission lines are in the red region at about 2.03 eV (610 nm), which is within the range of the CL band of the GeO₂ nanowires. CL spectrum of the Eu-doped GeO₂ nanowires is shown in Figure 3. A sharp Eu³⁺ line at

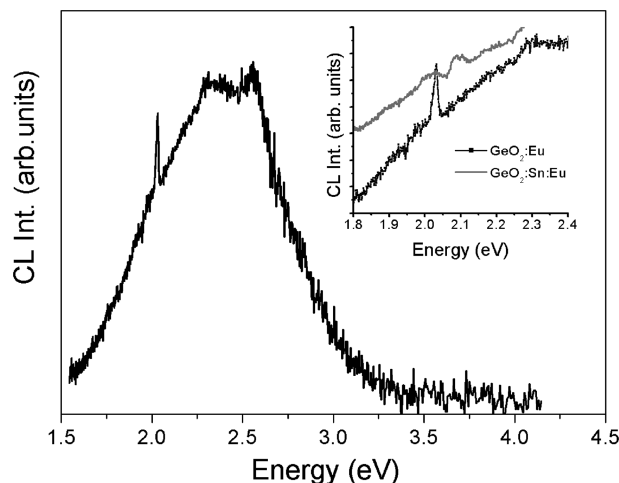


Figure 3. CL spectra of Eu-doped GeO_2 nanowires. Inset: Room temperature detailed CL spectra of Eu-doped and Sn-codoped GeO_2 :Eu nanowires.

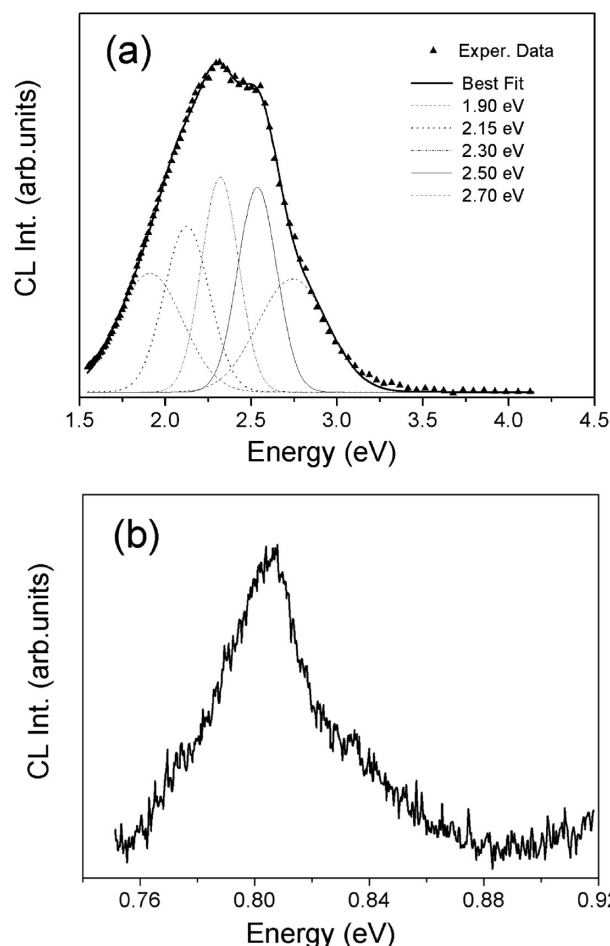


Figure 4. (a) Visible CL spectrum from Er-doped GeO_2 nanowires, showing the deconvoluted bands to fit the experimental results. (b) Infrared CL emission from the GeO_2 nanowires, showing the 0.80 eV erbium line.

2.03 eV is observed on the lower energy side in the spectrum. As mentioned above the presence of Sn codoping may also affect the luminescence features of the GeO_2 nanowires. The inset of Figure 3 shows the low-energy part of the spectra of Eu-doped and of the Eu,Sn-codoped nanowires. The sharp Eu^{3+} line at 2.03 eV (610 nm) observed in the Sn-free sample, appears as a broader bump in the codoped nanowires. Also in the

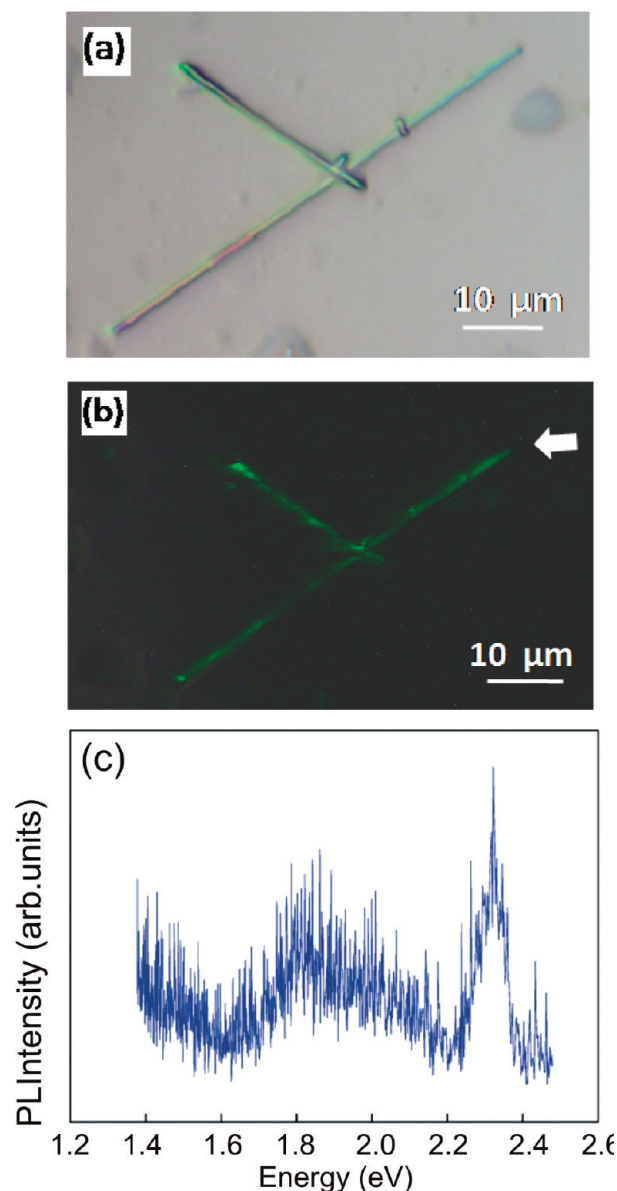


Figure 5. (a) Optical image of two crossing Er-doped microwires just placed one above another. (b) Dark field optical image of the path light through the wires. The source light comes into the right extreme of the lower wire as is indicated by the arrow and exit through both wires as it can be seen on the left ends of both wires. (c) μ -PL spectrum of the emergent light from the wire.

codoped nanowires, a small Eu^{3+} band at about 2.08–2.09 eV (590–595 nm) is observed. Lines at 2.03 and 2.08–2.09 eV correspond, respectively, to the $^5\text{D}_0$ – $^7\text{F}_2$ and $^5\text{D}_0$ – $^7\text{F}_1$ intraionic transitions of Eu^{3+} . It is well known that differences in the crystal field surrounding the rare earth ions result in slight shifts of their luminescence peaks or differences in their relative intensities.^{10,19} In this case, local changes in the Eu environment are caused by the Sn addition, which would lead to a modified local crystal field compared to Sn free wires. It is worth mentioning that Eu peaks are only detected at temperatures above 130 K. At lower temperatures the defects related band is very intense and the narrow Eu lines are not resolved in the spectrum.

Visible CL spectrum from Er-doped wires exhibits an intense broad green band as shown in Figure 4a. Deconvolution of the spectrum shows that a proper fit to the experimental curve is obtained when the 2.42 eV band, present in the spectra of the

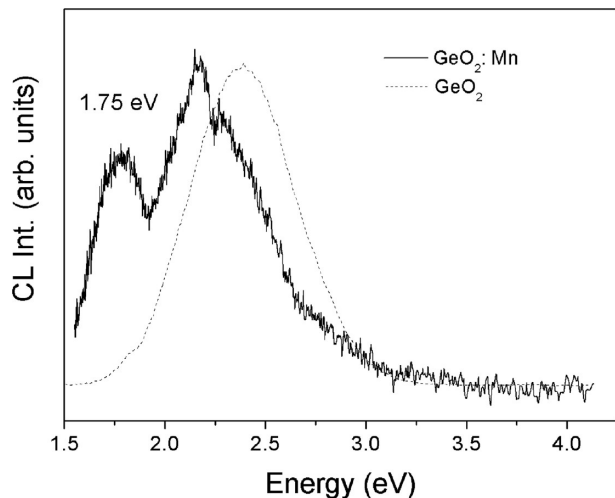


Figure 6. CL spectra from undoped (dashed line) and Mn-doped (solid line) GeO₂ nanowires. A new peak at 1.75 eV appears in Mn-doped samples.

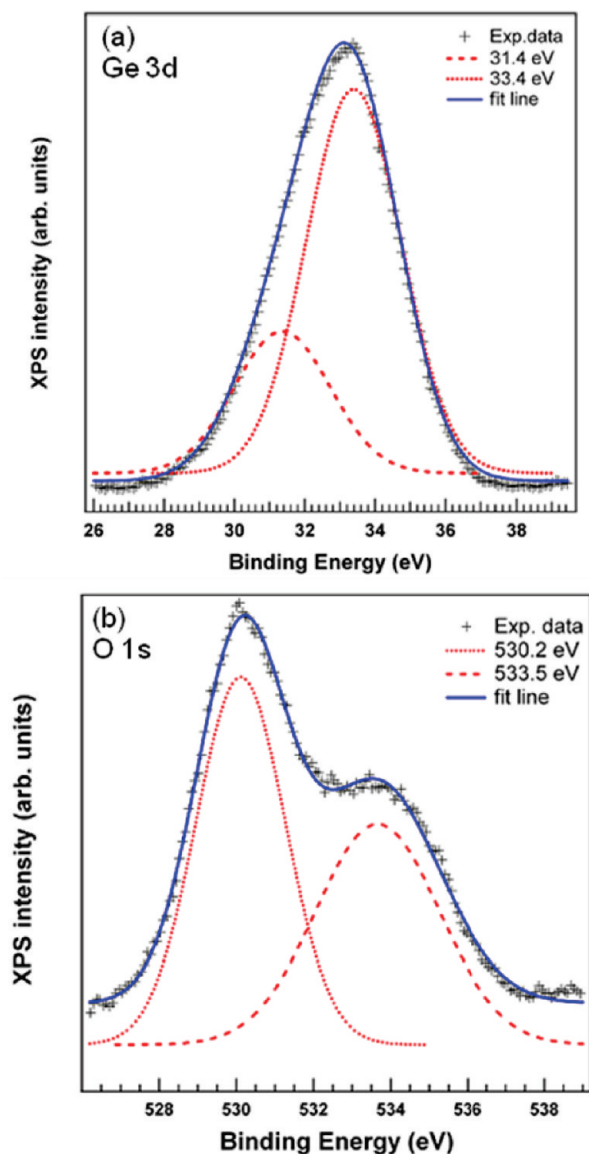


Figure 7. (a) Ge 3d and (b) O 1s XPS spectra of Mn-doped GeO₂ nanowires.

undoped nanowires, is split into two components (2.3 and 2.5 eV). The 2.3 eV (540 nm) energy corresponds to the known

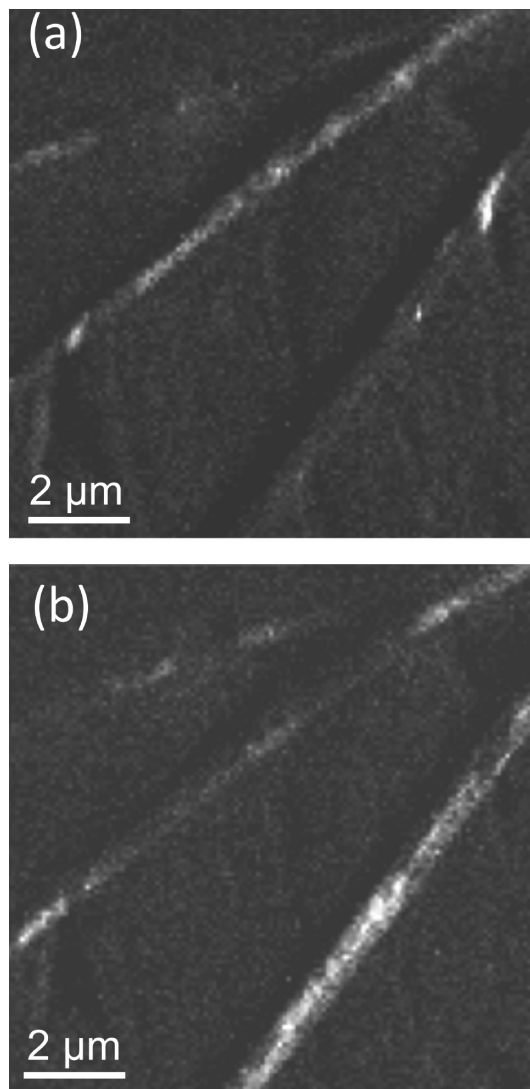


Figure 8. XPS images recorded the binding energy of Ge 3d core level at (a) 31.4 and (b) 33.4 eV.

green emission related to Er³⁺ ions. Hence, erbium doping leads to an increase of green emission of GeO₂ nanowires and no noticeable changes take place by Sn codoping. The luminescence mechanism in RE-doped semiconductors is usually due to an energy-transfer process between the host lattice and the RE ion.²⁰ In this case, since the main luminescence band of the host—GeO₂ nanowires—lies in the green region, a resonant excitation of the Er emission could take place leading to an increase of the total CL signal. Figure 4b shows the near-infrared CL spectrum of the nanowires with the 0.8 eV (1.54 μm) peak characteristic of Er³⁺ ions.

One of the potential applications of RE-doped nanowires is their use as waveguides in nanophotonic devices in a similar way that Er-doped silica fibers are widely used for this purpose in present optoelectronics. Undoped GeO₂ and Er-doped Ga₂O₃ nanowires have been demonstrated to behave as waveguides for visible light.^{2,21} Room temperature microphotoluminescence (μ-PL) measurements on Er-doped GeO₂ nanowires have been made in order to proof the waveguiding properties of these wires. Figure 5 shows the waveguide behavior of individual GeO₂ wires and an optical coupling phenomenon in two crossing wires. A green laser is used as source light and is pointed just in one end of the lower wire as indicated in the figure by an arrow. The light

travels through the wire, and a bright spot is clearly seen in the opposite wire end. Hence, light confinement and guiding through the wire is demonstrated. The light propagating along the lower wire is split at the crossing point of the wires and two green exit points are observed at the end of both wires, although the upper wire is not directly illuminated. One possible reason for this effect is that the evanescent field of the propagating light in one wire is coupled into the second wire at the crossing point leading to the light propagation in both wires.²² Another possible reason for the observed coupling is that the energy of the illuminating green laser excites luminescence bands in the GeO₂ nanowires in a resonant way. The excitation to the second wire would take place at the contact point of both wires. The μ -PL spectrum of the emergent light at the end of the wires, shown in Figure 5c, supports this possibility. The spectrum shows the green light from incident laser guided through the wire and a red band, which indicates that a luminescence process takes place. This red band may be associated to Er intraionic emissions, which are selectively excited by the incident green laser. These spectral measurements have been performed on single wires and at room temperature.

The other dopant, of GeO₂ nanowires, investigated was manganese, which is an impurity of interest in the field of diluted magnetic semiconductors. Manganese ions have been used in GaAs or GaN in order to achieve permanent magnetic moment in nonmagnetic semiconductor.²³ Also, transition metal ions may exhibit intrinsic luminescence properties due to the introduction of electronic levels in wide band gap semiconductors, see for example the role of Cr³⁺ ions in luminescence of Ga₂O₃ where the luminescence centers are coupled to the phonons of the host crystal by the electron–phonon interaction leading an intense red emission band.²⁴ Visible CL spectra from Mn-doped GeO₂ nanowires show a broad visible band composed by several peaks at 1.75, 2.15, 2.41, and 2.75 eV, as shown in Figure 6 (solid line). The three last peaks are present in undoped and Sn-doped GeO₂ wires and are associated with oxygen vacancy defects, while the 1.75 eV band was only observed in Mn doped samples. A red-shift of the emitted light, in doped nanowires, due to the increase of the 2.15 eV component is observed. The CL spectrum of undoped nanowires (dashed line) is also shown in the Figure 6, for comparison. Therefore, a modification of luminescence, with changes in the CL spectrum, has been detected by Mn doping of GeO₂ nanowires, probably due to electron–phonon interaction between the electronic levels of Mn atoms and the host crystal.

XPS measurements have been performed in order to achieve a deeper understanding of the luminescence bands in GeO₂ nanowires. Ge (3d) and O (1s) core levels have been measured in Er-doped and Mn-doped GeO₂ nanowires, while neither Er nor Mn peaks were observed at the probed surface. However, Sn is detected at the wires surface in codoped samples leading to a single-component peak related to the 3d level. XPS analysis of Mn-doped GeO₂ nanowires reveals that Ge (3d) and O (1s) peaks have several components, indicating the presence of several oxidation states of Ge. Figure 7a shows the Ge (3d) peak profile in a nanowire deconvoluted into two components, Ge²⁺ (BE = 31.4 eV) and Ge⁴⁺ (BE = 33.4 eV), that corresponds to the oxide species GeO and GeO₂.²⁵ O (1s) core levels also reveal the presence of Ge suboxides at the nanowire surface (Figure 7b). According with the literature, a low binding energy at 530.8 eV and a high-binding-energy component at 532.4 eV

have been found in the XPS O(1s) core level spectrum after oxidation process of Ge wafers.²⁶ The authors attributed these components to the presence of GeO and GeO₂, respectively. In this work, XPS images recorded with Ge and O binding energies in Mn-doped GeO₂ nanowires reveal that the wires are not completely homogeneous and certain mixture of oxides is present in the surface. Figure 8 shows XPS images of two nanowires recorded at the Ge binding energies of 31.4 and 33.4 eV. The images show complementary contrast, which shows the presence of GeO and GeO₂ in different wires. This effect is limited to the surface, while the crystal structure of the wires is that of GeO₂ as measured by XRD. This feature would be the responsible for the complex visible luminescence bands observed in doped GeO₂ nanowires. The growth process involves thermal oxidation of an initial Ge–metal oxide mixture and the presence of several species may affect the final oxidation state of germanium oxide. On the other hand, electronic states related to oxygen vacancies may also contribute in a different way depending on the Ge oxide. The addition of impurities may slightly influence the Ge 3d and O 1s core energy levels leading to a different contribution of the luminescence bands in the CL spectra, as observed.

In summary, GeO₂ micro- and nanowires doped with Er, Eu, or Mn have been obtained by a catalyst-free thermal evaporation–deposition method in a single-step approach. Sn codoping of GeO₂ nanowires prevents or reduces, in all studied cases, the formation of sharp bends in the wires. This makes the wires more useful for waveguiding applications. Optical coupling of Er-doped GeO₂ nanowires acting as waveguides of green laser light has been demonstrated. RE ions (Eu and Er) show their characteristic emission lines in the nanowires with a rather high efficiency, even at room temperature, and Mn impurities originate a luminescence band at 1.75 eV not observed in the other doped or undoped nanowires. The complex visible luminescence band in doped GeO₂ nanowires has been discussed in relation with the presence of impurities and native defects. XPS shows the presence of GeO in the surface of some nanowires.

Acknowledgment. This work has been supported by MEC (Project MAT 2006-01259). The authors are grateful to Dr. Luca Gregoratti at the Sincrotron Trieste for useful advises on XPS measurements.

References and Notes

- (1) Law, M.; Sirbuly, D. J.; Johnson, J. C.; Goldberger, J.; Saykally, R.; Yang, P. D. *Science* **2004**, *305*, 1269.
- (2) Hidalgo, P.; Méndez, B.; Piqueras, J. *Nanotechnology* **2007**, *18*, 155203.
- (3) Palm, J.; Gan, F.; Zheng, B.; Michel, J.; Kimerling, L. C. *Phys. Rev. B* **1996**, *54*, 17603.
- (4) Priolo, F.; Franzò, G.; Pacifici, D.; Vinciguerra, V.; Iacona, F.; Irrera, A. J. *Appl. Phys.* **2001**, *89*, 264.
- (5) Heikenfeld, J.; Garter, M. J.; Lee, D. S.; Birkhahn, R. H.; Steckl, A. J. *Appl. Phys. Lett.* **1999**, *75*, 189.
- (6) Lozykowski, H. J.; Jadwisieniczak, W. M.; Han, J.; Brown, I. G. *Appl. Phys. Lett.* **2000**, *77*, 767.
- (7) Peng, H.; Lee, C. W.; Everitt, H.; Munasinghe, C.; Lee, D. S.; Steckl, A. J. *Appl. Phys.* **2007**, *102*, 073520.
- (8) Strohhöfer, C.; Capecci, S.; Fick, J.; Martucci, A.; Brusatin, G.; Guglielmi, M. *Thin Solid Films* **1998**, *326*, 99.
- (9) Wu, J.; Coffey, J. L.; Wang, Y.; Schulze, R. *J. Phys. Chem. B* **2009**, *113*, 12.
- (10) Nogales, E.; Méndez, B.; Piqueras, J.; García, J. A. *Nanotechnology* **2009**, *20*, 115201.
- (11) Ishizumi, A.; Kanemitsu, Y. *Appl. Phys. Lett.* **2005**, *86*, 253106.
- (12) Wu, J.; Coffey, J. L. *Chem. Mater.* **2007**, *19*, 6266.

- (13) Hidalgo, P.; Méndez, B.; Piqueras, J. *Nanotechnology* **2008**, *19*, 455705.
- (14) Fitting, H. J.; Barfels, T.; Trukhin, A. N.; Schmidt, B. *J. Non Cryst. Solids* **2001**, *259*, 51.
- (15) Nogales, E.; Montone, A.; Cardinelli, F.; Méndez, B.; Piqueras, J. *Semicond. Sci. Technol.* **2002**, *17*, 267.
- (16) Kartopu, G.; Bayliss, S. C.; Hummel, R. E.; Ekinci, Y. *J. Appl. Phys.* **2004**, *95*, 3466.
- (17) Oku, T.; Nakayama, T.; Kuno, M.; Nozue, Y.; Wallenberg, L. R.; Niihara, K.; Suganuma, K. *Mater. Sci. Eng. B.* **2000**, *74*, 242.
- (18) Singha, A.; Roy, A.; Kabiraj, D.; Kanjilal, D. *Semicond. Sci. Technol.* **2006**, *21*, 1691.
- (19) Dierolf, V.; Sandman, C.; Zavada,.; Chow, P.; Herzog, B. *J. Appl. Phys.* **2004**, *95*, 5464.
- (20) Polman, A. *J. Appl. Phys.* **1997**, *82*, 1.
- (21) Nogales, E.; García, J. A.; Méndez, B.; Piqueras, J. *Appl. Phys. Lett.* **2007**, *91*, 133108.
- (22) Voss, T.; Svacha, G. T.; Müller, S.; Ronning, C.; Konjhodzic, D.; Marlow, F.; Mazur, E. *Nano Lett.* **2007**, *7*, 3675.
- (23) Keavney, D. J.; King, S. T.; Cheung, S. H.; Weinert, M.; Li, L. *Phys. Rev. Lett.* **2005**, *95*, 257201.
- (24) Nogales, E.; García, J. A.; Méndez, B.; Piqueras, J. *J. Appl. Phys.* **2007**, *101*, 033517.
- (25) Molle, A.; Bhuyian, M. N. K.; Tallarida, G.; Fanciulli, M. *Appl. Phys. Lett.* **2006**, *89*, 083504.
- (26) Prabhakaran, K.; Ogino, T. *Surf. Sci.* **1995**, *325*, 263.

JP905587C